Prediction of Percutaneous Penetration

Methods, Measurements, Modelling

VOLUME 2

Proceedings of the conference held in April, 1991

Edited by
R C Scott, R H Guy, J Hadgraft and H E Boddé

Associate Editor
S M Tittensor

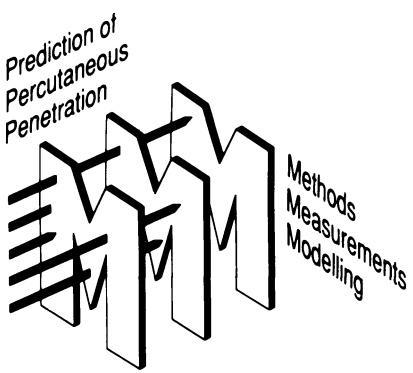

IBC Technical Services

A method for the prediction of *in vivo* blood levels during application of matrix-type and membrane-controlled-type transdermal delivery devices

A Göpferich, G Lee

Institute for Pharmaceutical Technology and Biopharmaceutics, Heidelberg University, Im Neuenheimer Feld 366, 6900 Heidelberg, Germany

Introduction

The development of a transdermal delivery device for a drug can be a rather complicated and time-consuming task. The drug itself must obviously first show physicochemical properties propitious for topical delivery, eg low daily dosage and good skin permeability. The Galenical problem is then primarily that of developing a device that on application to the skin *in vivo* yields a satisfactory drug plasma profile. The important properties of the device in this respect are the rate, extent and duration of drug release. For the case of a matrix-type device, these can be adjusted in some measure by modifying matrix thickness, drug loading and drug diffusivity within the matrix. The drug release rate from a membrane-controlled device depends on drug loading of the reservoir, thickness of the rate-controlling membrane, drug diffusivity within the rate-controlling membrane, and the size of any loading dose present. The drug release properties of either type of device can readily be determined by *in vitro* experiment. An *in vivo* study can be undertaken to determine the drug plasma and urinary excretion profiles obtained from the device. At this stage, the formulator may well be interested in predicting how alterations in the Galenical properties of the device or changes in the permeability of the skin would influence these *in vivo* profiles. For the successful prediction of these effects, a model is required that describes — with suitable exactitude — the physicochemical and biological processes involved. Much advance has been made in this field of pharmaceutical research during the last ten years. Both compartmental[1] and combined diffusion/compartmental[2,3] models of varying complexity have been proposed. In this paper we relate how basic models for the prediction and evaluation of transdermal drug delivery have been developed using a simple numerical technique.

Model description and evaluation

As recognized some years ago,[4] the morphological problem of transdermal drug delivery can be represented by a multilayer model of the type illustrated in Figure 1. The outermost, left-hand layer (B) represents the delivery device, which is attached

in some way to the outer surface of the skin (C). The drug present within the device is released at a rate dependent on the device's structure and properties. The physicochemical processes of first importance here are passive diffusion of the drug and its partitioning at any boundaries where the properties of the medium change, eg at x=C, between the device and the outermost skin layer. The kinetics of partitioning may also need to be considered.[5] The stratum corneum, together with any surface lipid, is represented by the second layer of the model (D). Although this tissue has an intricate internal structure, the simplification that it behaves as an isotropic layer has been successfully applied to numerous quantitative studies of drug transport through skin. Passive diffusion is again the important process within this layer, although others, such as sorption of the drug, may also occur. The viable epidermis is represented by the next layer of the model (F), as it is known to form a morphologically distinct layer within the skin.[6] Partitioning must be considered at the plane E, together with passive diffusion within the viable epidermis itself. The treatment of this layer as a compartment can be justified, however, since its resistance to the diffusional movement of drug molecules is many times less than that of the adjacent stratum corneum. Thus, although the drug arrives slowly at the outermost side of the viable epidermis (E), it then diffuses very rapidly through this layer as a consequence of its high permeability. The drug concentration within the viable epidermis can, therefore, be considered as being the same everywhere, ie as being only a function of time. The next morphological layer of the skin is the dermis. Because this tissue contains an extensive network of capillaries extending up to the junction with the viable epidermis, it can be combined with the blood as a

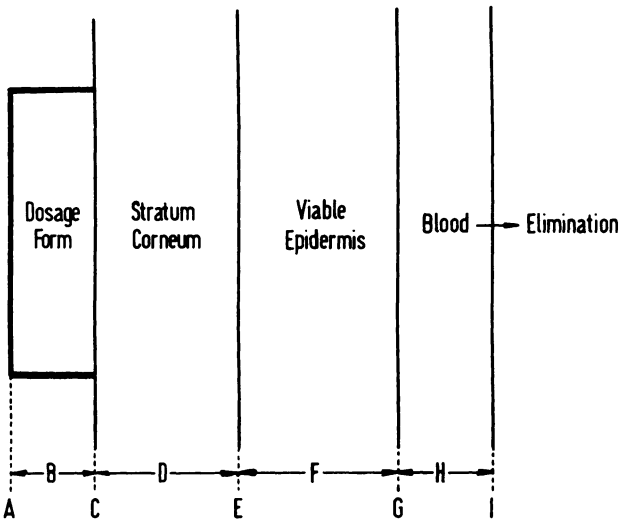

Figure 1 Multilayer representation of transdermal drug delivery.

single compartment (H). Once present within the blood, the drug may be distributed into the peripheral tissues and will be eliminated.

Each layer of this scheme has characteristic drug transport properties which differ substantially from those of the neighbouring layers. It is therefore possible to characterize drug transport within an individual layer by examination of the physicochemical processes occurring there. For example, it is relatively easy to measure drug transport within either of the two outer layers of the model, namely, the delivery device and the stratum corneum. Once knowledge of the drug transport properties of the individual layers is available, a basic model can be assembled to describe the complete process of transdermal drug delivery, as represented by the scheme in Figure 1. We start by considering measurement of drug transport within excised human stratum corneum and a matrix-type delivery device.

Model I: stratum corneum

Isolated sheets of human stratum corneum can be readily prepared from whole skin excised from cadavers.[7] The transport properties of a drug within this tissue can be characterized by measuring its permeation from a donor medium through the tissue and into an acceptor medium. A diffusion cell of some standard design[8] can be used. For the model discussed here, the stratum corneum will exist in the hydrated state. The standard representation of this diffusional problem is given in Figure 2 for an assumed isotropic sheet of stratum corneum of thickness h. The drug concentration within the stratum corneum, $c_{sc}(x,t)$, is given as a function of space, x, and time, t, by Fick's second law. Provided the ratio of radius to thickness of the sheet (r/h) is > *ca* 100, linear diffusion can be assumed:

$$D_{sc} \cdot c_{sc}(x,t)_{xx} - c_{sc}(x,t)_t = 0, \quad 0<x<h, \quad t>0, \tag{1}$$

where D_{sc} is the drug diffusivity within the stratum corneum (cm^2sec^{-1}). The subscripts x and t denote the respective partial derivatives. Initially, the drug is contained within the donor medium:

$$c_d(0) = c_o, \quad c_a(0) = 0, \tag{2}$$

$$c_{sc}(x,0) = 0, \quad 0 \leq x \leq h. \tag{3}$$

The non-sink transport of drug at the two boundaries is given by Fick's first law:

$$m_a'(t) = D_{sc} \cdot c_{sc}(0,t)_x, \quad t>0, \tag{4}$$

$$m_a'(t) = D_{sc} \cdot c_{sc}(h,t)_x, \quad t>0, \tag{5}$$

where m(t) denotes drug mass and a′ a first ordinary derivative. The drug concentration in the acceptor is given by:

$$c_a(t) = c_{sc}(h,t)/K, \quad t>0, \tag{6}$$

where K is the drug's partition coefficient between stratum corneum and acceptor medium. The analytical solution to this problem[9] is an awkward transcendental function, not particularly convenient for the evaluation of experimental data. A more flexible way of treating it is to employ the numerical analysis developed by Crank and Nicolson especially for solving partial differential equations of the diffusion type.[10] Equations 1–6 are expressed in finite differences to yield algebraic approximations in the form of a tridiagonal matrix. The solution can be obtained by Gauss' elimination method and programmed in Pascal on a personal computer. It is advisable to have the capacity of at least an 80 386 processor with 80 387 co-processor.

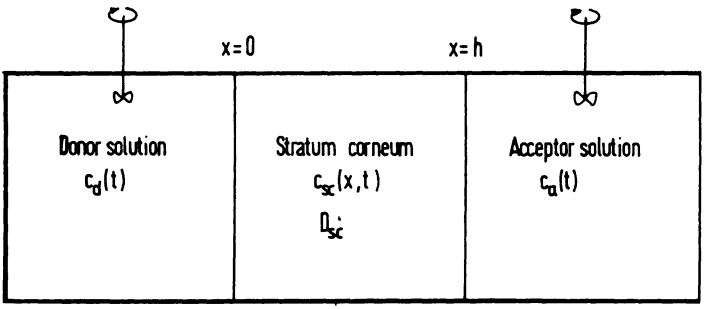

Figure 2 Diffusional model for drug permeation through an excised stratum corneum membrane.

The programme can be used to simulate drug permeation through an isolated sheet of stratum corneum, showing how the parameters diffusivity, membrane thickness and partition coefficient influence the drug concentration profile within the stratum corneum, $c_{sc}(x,t)$, and the profile of drug mass in the acceptor, $m_a(t)$.[11] Additionally, it is possible to calculate the diffusivity and partition coefficient from experimental data. Figure 3 shows an example of some experimentally determined co-ordinates of $m_a(t)$, obtained for the permeation of the basic drug clenbuterol (MW=277, pk_a=9.5) through excised human stratum corneum. The typical permeation profile is seen. The curve passing through these co-ordinates is the numerical solution to Equations 1–6 which best fits the data, as determined by Nelder and Mead's improved simplex method.[12] Although not obvious to the eye, the fitted curve is sigmoidal in shape, as a result of the prevailing non-sink boundary conditions. The point of inflexion occurs after *ca* 60 hours, which corresponds to a value of 0.023 for $m_a(t)/m_o$. Thus, the point of maximum flux is reached when only 2.3% of the drug has arrived in the acceptor. Detailed investigations showed that the accuracy of the $m_a(t)$ values in this case was such that a weighting factor need not be used at the short times. The curve fit gives a diffusivity of $3.97\times10^{-12} \pm 2.33\times10^{-12}$cm^{2}sec^{-1} and a partition coefficient of 212 ± 165(n=6).

The large standard deviations can be taken to arise from two sources: firstly, natural variation in the anisotropic nature of the stratum corneum, and, secondly, error in the determination of the thickness of the stratum corneum. Much less scatter is found with permeation measurements made on an isotropic silicone membrane of known thickness, for example, with coefficients of variation of 5% for diffusivity and 12% for partition coefficient. These variations can be fully accounted for by experimental error in the determination of c_0 and $m_a(t)$. Equation 1 is, strictly speaking, not applicable to stratum corneum. The simplest attempts to overcome the problem of anisotropy involve retaining Equation 1, and making purely algebraic calculations based on the geometry of a 'bricks-and-mortar' representation of the microstructure of the stratum corneum.[13,14] The derivation of a comprehensive diffusional model for the stratum corneum based on solutions to Fick's second law represents a formidable, yet challenging, mathematical task. Although a model of such intricacy would be intellectually more satisfying, it remains to be seen if it would offer any practical advantage over the simple assumption of isotropy within the stratum corneum.

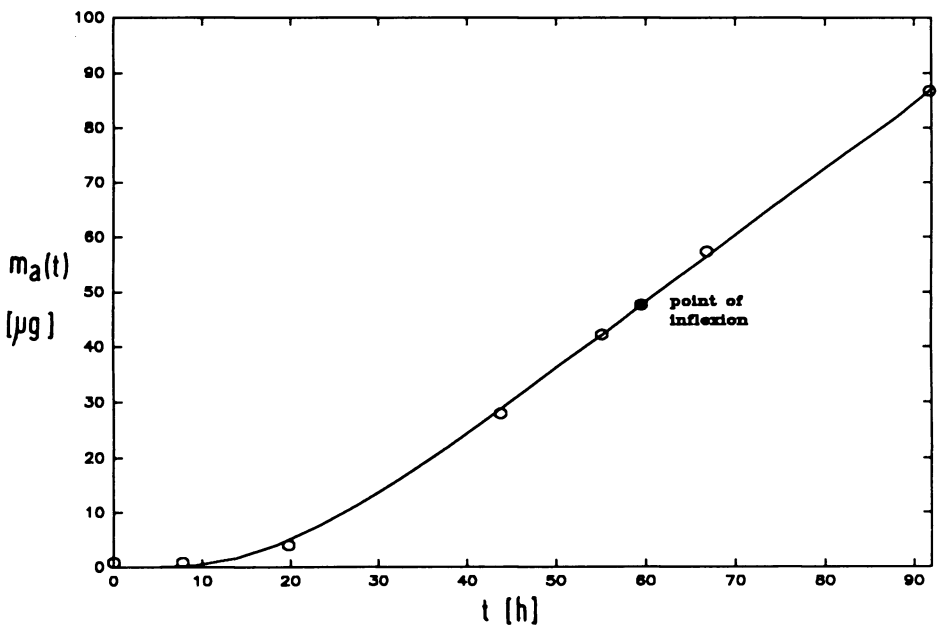

Figure 3 Fit of experimental co-ordinates of $m_a(t)$ for clenbuterol permeation through excised human stratum corneum to numerical model (curve).

Model II: polymer matrix

The transport properties of a drug within a polymeric matrix of thickness L, intended for use as a transdermal delivery device, can be conveniently obtained from measurement of the rate of drug release into an adjacent acceptor medium. For a thin matrix (r/h>*ca* 100), the standard representation shown in Figure 4 can again

be characterized by the linear form of Fick's second law:

$$D_m.c_m(x,t)_{xx} - c_m(x,t)_t = 0, \quad -L<x<0, \ t>0, \tag{7}$$

where $c_m(x,t)$ is the drug concentration within the matrix and D_m its diffusivity. The drug is initially homogeneously dissolved within the matrix:

$$c_m(x,0) = c_o, \quad -L \leq x \leq 0, \tag{8}$$

$$c_a(0) = 0. \tag{9}$$

The outer, left-hand side of the matrix is insulated, and the drug is released at x=0 into a non-sink:

$$c_m(-L,t)_x = 0, \ t>0 \tag{10}$$

$$ma(t)' = -D_m.c_m(0,t)_x, \ t>0. \tag{11}$$

The drug concentration in the acceptor is governed by:

$$c_a(t) = c_m(0,t)/K', \tag{12}$$

where K′ is the drug's partition coefficient between matrix and acceptor medium.

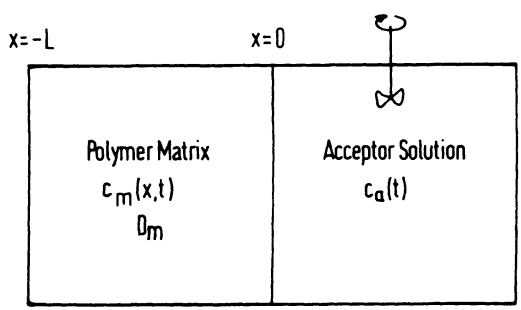

Figure 4 Diffusional model for drug release from a rectangular polymer matrix.

Numerical analysis of this problem is again more flexible than use of the analytical solution,[15] and yields simulated release profiles of $m_a(t)$ as a function of diffusivity, matrix thickness and partition coefficient.[11] Figure 5 shows an example of experimentally determined co-ordinates of $m_a(t)$ for the release of clenbuterol from a thin (50μm) matrix prepared from a purified form of Eudragit NE30D (Röhm Pharma). Again, the curve is the numerical solution to Equations 7–12

which best fits the data. The fitted diffusivity of $9.31 \times 10^{-12} \pm 0.7 \times 10^{-12} cm^2 sec^{-1}$ (n=4), for a drug loading of 8% w/w, has a coefficient of variation of *ca* 7%, which can be accounted for solely by experimental error in the determination of c_0 and $m_a(t)$. The former is most accurately determined from the weight ratio of drug to polymer used for the preparation of the matrix by (in this case) solvent evaporation. Difficulties arise with the fitting of the best value for a partition coefficient. The values obtained show enormous variation, some being quite unrealistically large. The matrix comprising the finite-difference forms of Equations 7–12 is undoubtedly non-singular, implying the existence of unique values for both D and K′. The failure to fit K′ is caused by its extremely small influence on the release profiles generated with the model. Thus, immediately t becomes greater than zero, the drug concentration within the outermost layer of the matrix falls sharply in accordance with the assumption of spontaneous partitioning at x=0 implicit in Equations 11 and 12. This results in very small values for $c_a(t)$ in the case of matrix/acceptor partition coefficients > 1. Because $c_a(t)$ is so small, K′ exerts negligible influence on the concentration gradient in Equation 11, and hence the release rate. This insensitivity to K′ makes the D/K′-simplex plane very flat in the K′-direction. For values of K′ in excess of *ca* 100, the curve-fit cannot converge sharply on K′, despite converging well on D. The measured matrix/buffer partition coefficient for clenbuterol is 120. This is, indeed, a known problem with the Nelder-Mead method.[12]

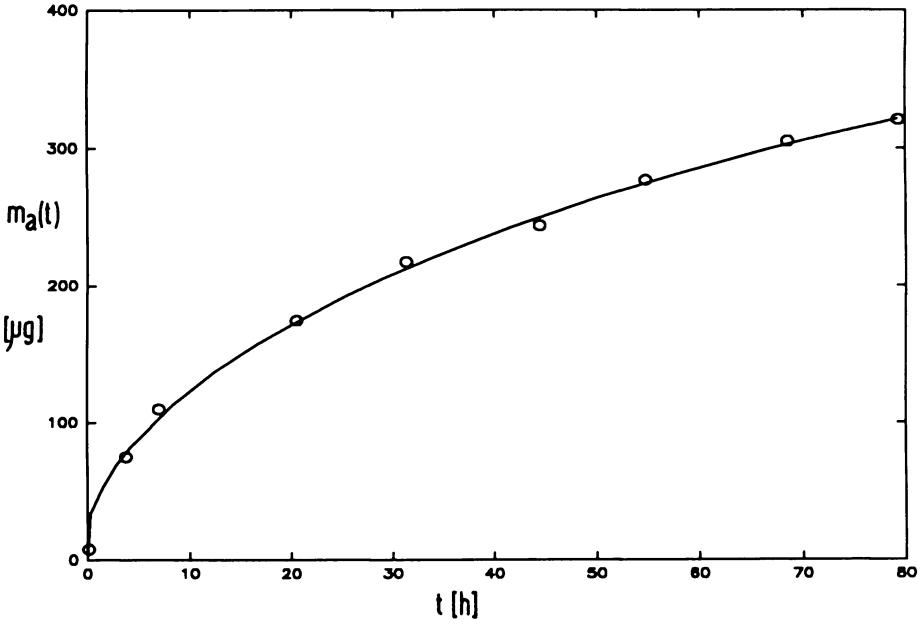

Figure 5 Fit of experimental co-ordinates of $m_a(t)$ for clenbuterol release from a purified Eudragit NE30D matrix to numerical model (curve).

Model III: transdermal delivery from a matrix-type device

This model directly links the transport properties of the device and the stratum corneum (ie Models I and II above) to the drug plasma and urinary excretion profiles obtained during topical application of the device. It can be viewed as a somewhat refined version of a combined diffusion/compartmental model presented by Tojo.[2] It has the advantage over previous models in that it is not necessary to specify particular drug release kinetics from the device or to assume the existence of steady-state or sink conditions. The two-dimensional representation is shown in Figure 6. The release of drug from the matrix of thickness L, and its subsequent permeation through the stratum corneum of thickness h, are governed by the linear form of Fick's second law. For the matrix, this involves the use of Equations 7, 8 and 10; for the stratum corneum, Equations 1 and 3 are required. These two layers are in perfect diffusional contact at x=0:

$$D_m.c_m(0,t)_t = D_{sc}.c_{sc}(0,t)_t, \quad t > 0. \tag{13}$$

Owing to the very low diffusional resistances existing within the underlying tissues, each is represented by a compartment. This results in a three-compartment model with five first-order rate constants, joined at x=h to the double diffusion layer:

$$b.c_e'(t) = -D_{sc}.c_{sc}(h,t)_x, \tag{14}$$

where $c_e(t)$ is the drug concentration in the viable epidermis/dermis compartment of 'thickness' b. The drug mass in the plasma, $m_p(t)$, is then given by:

$$m_p'(t) = k_{12}.m_e(t) - \{k_{21}+k_e+k_{23}\}.m_p(t)+k_{23}.m_t(t), \tag{15}$$

and the eliminated mass, $m_u(t)$, by:

$$m_u'(t) = k_e.m_p(t). \tag{16}$$

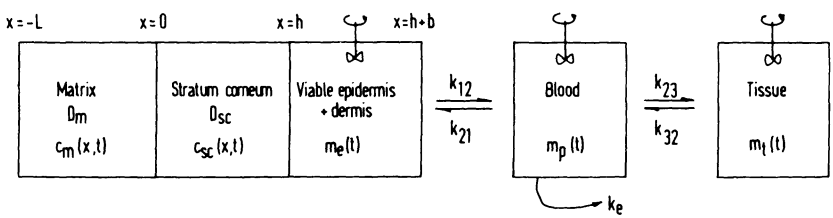

Figure 6 Model for transdermal drug delivery from a matrix-type device.

The numerical solution programmed in Pascal can be used to evaluate *in vivo* data and obtain values for those system constants that cannot be determined from independent experiments, ie k_{12} and k_{21}. It can also be used to simulate the effects of the system parameters on the drug plasma profile, eg drug diffusivity within matrix and stratum corneum, and drug loading and thickness of the matrix.[3] A simulation for clenbuterol using the values obtained for D_m and D_{sc} from the first two models yields, however, the rather unsatisfactory drug plasma profile shown in Figure 7 (lower curve). It does not reach a maximum after an application time of seven days; this finding does, however, agree with *in vivo* data obtained during the transdermal application of this drug from a polymer matrix.[3] This is certainly due to the drug's long half-life. A simulated 5-fold increase in D_{sc} — as could feasibly be achieved for this drug with Azone^R — does not greatly improve the profile (upper curve in Figure 7). Indeed, only an extension of the simulation time to 28 days (insert to Figure 7) shows how a maximum in the plasma profile is first reached at a t_{max} of *ca* 21 days.

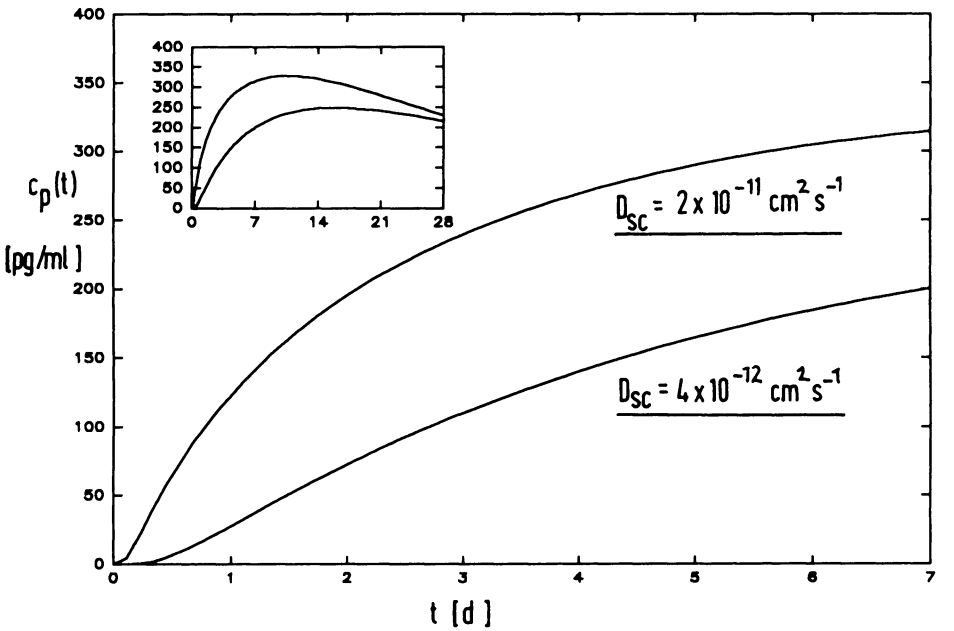

Figure 7 Simulated drug plasma profiles for transdermal drug delivery from a matrix-type device (D_m=9.3×10^{-12}cm^{2}sec^{-1}; D_{sc}=4×10^{-12}cm^2 sec^{-1} (lower curve), D_{sc}=2×10^{-11} cm^2 sec^{-1} (upper curve); c_o = 1.25mg/2cm^2; K=1; K′=1; L=68μm; h=15μm; b=50μm; k_{12}=2h^{-1}; k_{21}=12h^{-1}; k_{23}=0.2h^{-1}; k_{32}=0.5h^{-1}; k_e=0.028h^{-1}; A=2cm^2; V_d=90l). Insert: extended simulation up to 28 days for D_{sc}=4×10^{-12} (lower curve) and 2×10^{-11} (upper curve) cm^2 sec^{-1}.

Model IV: transdermal delivery from a membrane-controlled device

It may be possible to reduce the predicted t_{max} of 21 days for transdermal clenbuterol by incorporating a 'loading dose' of drug into the system. This can best be illustrated for the case of a membrane-controlled transdermal device, necessitating a slight modification to Model III. Thus, the two outer layers of the scheme shown in Figure 8 now represent the device, comprising a drug reservoir, in which the drug concentration is only time-dependent, enclosed by a rate-controlling membrane of thickness a. The membrane will contain an initial loading dose of drug (ie $c_{me}(x,0)>0$) as a result of the partitioning equilibrium at x = –a (partition coefficient = K_1). Non-sink transport of the drug occurs at this boundary:

$$m_r(t)' = D_{me}.c_{me}(-a,t)_x, \quad t>0, \tag{17}$$

where $m_r(t)$ is drug mass within the reservoir and $c_{me}(x,t)$ is the drug concentration within the membrane. Upon application of the device to the skin (at t=0), the drug partitions at x=0 from the membrane into the stratum corneum (partition coefficient = K_2) and diffuses up to the boundary with the viable epidermis/dermis compartment. Within the rate-controlling membrane:

$$D_{me}.c_{me}(x,t)_{xx} - c_{me}(x,t)_t = 0, \quad -a<x<0, \quad t>0, \tag{18}$$

where D_{me} is the drug diffusivity. The boundary condition at x=0, between rate-controlling membrane and stratum corneum, describes perfect diffusional contact:

$$D_{me}.c_{me}(0,t)_t = D_{sc}.c_{sc}(0,t)_t, \quad t>0. \tag{19}$$

Equation 1 is valid for the stratum corneum. The boundary condition at x=h, between stratum corneum and the viable epidermis/dermis compartment, is the same as Equation 14. The three-compartmental part is identical to that for Model III, with the drug plasma and urinary excretion profiles again being given by Equations 15 and 16, respectively.

The numerical solution to the complete model enables calculations to be made for a device having a rate-controlling membrane made of the same polymer as the matrix, namely, Eudragit NE30D. The drug plasma profiles shown in Figure 9 were thus all simulated for a membrane diffusivity of $1\times10^{-11}cm^2sec^{-1}$, a membrane thickness of 10μm, and a membrane/lipoid-reservoir partition coefficient, K_1, of 0.1. The lowest curve represents an initial drug concentration in the reservoir, $c_r(0)$, of $10mgcm^{-3}$ (all dissolved; no suspended drug present), which produces, by virtue of equilibrium partitioning at x = –a, an initial drug loading in the membrane, $c_{me}(x=0)$, of $1mgcm^{-3}$, ie $c_r(0)/c_{me}(x,0)=0.1$. This plasma profile is, however, no better than those profiles seen for the matrix system in Figure 7. Yet, by holding $c_r(0)$ and K_1 constant, and artificially increasing $c_{me}(x,0)$ to $10mgcm^{-3}$ (top curve in Figure 9), a much more promising drug plasma profile is obtained. The t_{max} is

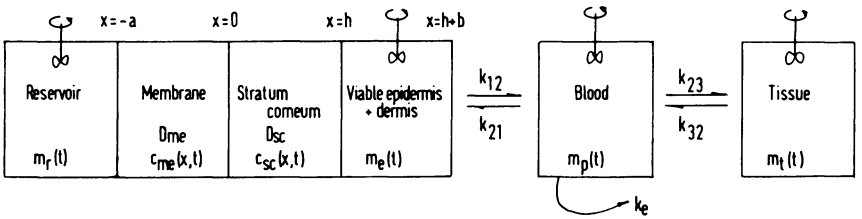

Figure 8 Model for transdermal drug delivery from a membrane-controlled device.

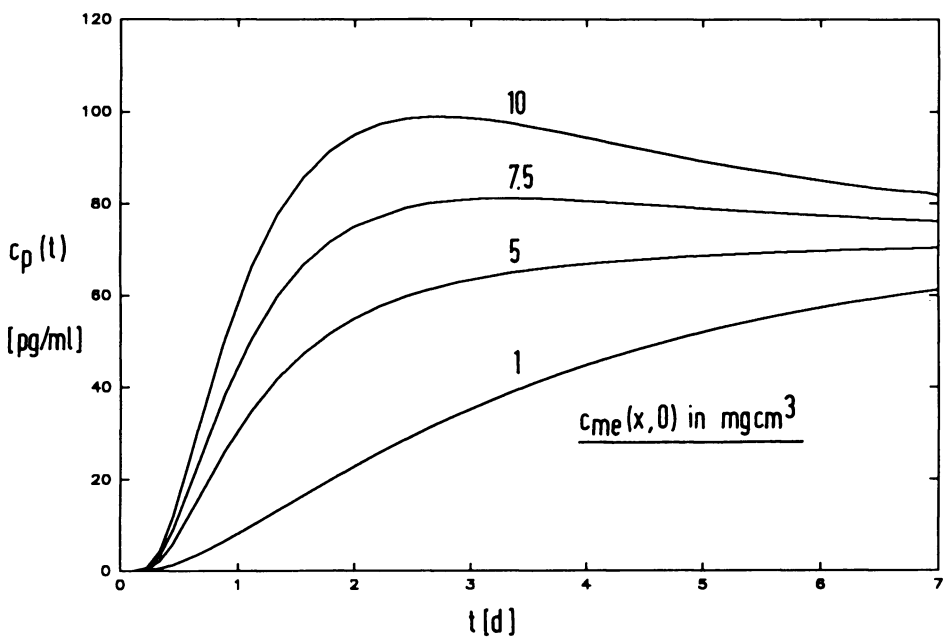

Figure 9 Simulated drug plasma profiles for transdermal drug delivery from a membrane-controlled device ($c_r(0)$=10mgcm^{-3}; K_1=0.1; D_{me}=9.3×10^{-12} cm^2 sec^{-1}; $c_{me}(x,0)$=1mgcm^{-3} (lower curve), $c_{me}(x,0)$=10mgcm^{-3} (upper curve); all compartmental constants as given in Figure 7).

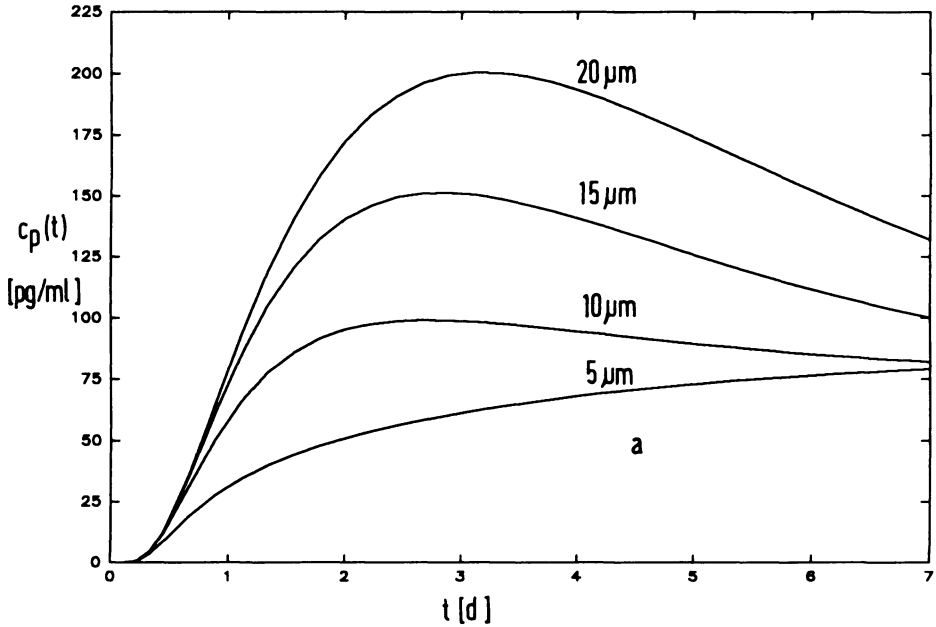

Figure 10 Effect of membrane thickness on simulated drug plasma profiles for transdermal drug delivery from a membrane-controlled device ($c_{me}(x,0)=10 mgcm^{-3}$; all other constants as given in Figure 9).

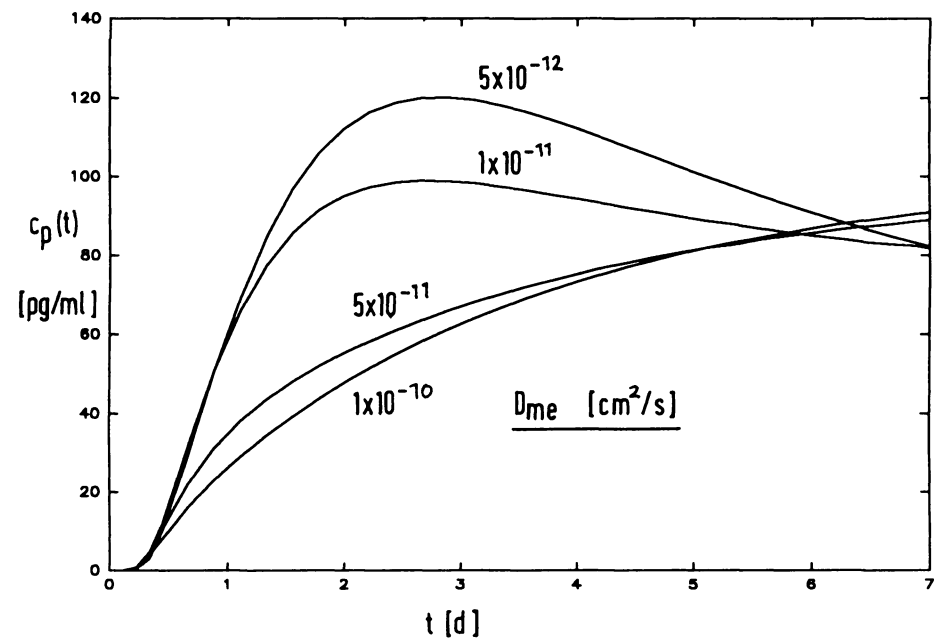

Figure 11 Effect of diffusivity within membrane on simulated drug plasma profiles for transdermal drug delivery from a membrane-controlled device ($c_{me}(x,0)=10 mgcm^{-3}$; a=10µm; all other constants as given in Figure 9).

reduced to *ca* 2.5 days, a value comparable with that found for the transdermal application of a clonidine TTS.[16] Additionally, c_{max} lies within the correct therapeutic range for clenbuterol, of *ca* 100pgml^{-1}. It must be remembered, however, that this loading dose of 10mgcm^{-3} is in excess of that arising purely from equilibrium partitioning between reservoir and membrane (ie only 1mgcm^{-3}). A special design would, therefore, be required for the device, to prevent the excess loading dose partitioning backwards into the reservoir upon storage. An interesting effect can be observed by altering membrane thickness whilst retaining a $c_{me}(x,0)$ of 10mgcm^{-3}; by halving the membrane thickness from its original 10μm to 5μm (Figure 10), the drug plasma profile becomes much flatter and t_{max} increases greatly. Although $c_{me}(x,0)$ is the same for all membrane thicknesses, a thinner membrane contains less drug mass, thereby effectively reducing the loading dose and nullifying its beneficial effects on the drug plasma profile. An increase in thickness above 10μm raises the drug plasma profile, but also increases t_{max}. In these cases, it takes a longer time to reach the higher c_{max}, since all diffusivities and partition coefficients within the system remain the same. Increasing the diffusivity within the rate-controlling membrane from 1×10^{-11} to 1×10^{-10}cm^{2}sec^{-1}, whilst keeping a $c_{me}(x,0)$ of 10mgcm^{-3} and a thickness of 10μm, decreases the drug plasma profile over the first six days (Figure 11). This effect is also related to a detrimental influence on the loading dose. Thus, by increasing D_{me}, not only is the forward diffusion at x=0 into the stratum corneum accelerated, but also the backward diffusion of the loading dose at x = –a into the drug reservoir. The beneficial influence of the loading dose is thereby nullified once more.

Conclusion

The two models discussed here for transdermal drug delivery are clearly not comprehensive; various processes are not considered which may be of importance for the drug plasma profile, eg drug metabolism within the viable tissues, the presence of a resistive adhesive layer between matrix or membrane and the stratum corneum, or possible drug distribution into erythrocytes. It is a relatively straightforward matter to incorporate such processes into the numerical model, allowing further simulations to be made. It must, however, be recognized that the growing complexity of the models leads to an increase in the error associated with their use to evaluate experimental data. This is especially the case with *in vivo* data, where the experimental scatter is likely to be rather large.

Recognition of the anisotropic structure of the stratum corneum could lead to an interesting further development of Model I. *In vitro* experiments with skin lipids indicate that drug diffusivities within the lipid fraction of the stratum corneum are probably *ca* 10^{-8}cm^{2}sec^{-1}. Yet drug diffusivities calculated from permeation data through excised human stratum corneum are some 10^3–10^4 times smaller with the assumption of isotropicity. Calculations based on a simple bricks-and-mortar structure yield, however, multiplication factors of just this order, indicating that the outstanding barrier properties of the stratum corneum may be largely of geometrical origin. The critical factors are probably

the extended diffusional pathway across the thickness of the stratum corneum, and the very small effective diffusional area within the stratum corneum. It may also be of interest to examine the influence of non-spontaneous partitioning[5] for Models I and II.

References

1. Guy R, Hadgraft J, Maibach H, *Int J Pharm,* **11**, 119–129(1982).
2. Tojo K, *Int J Pharm,* **43**, 201–205(1988).
3. Göpferich A, Lee G, *Int J Pharm*, **71**, 237–243(1991).
4. Guy R, Hadgraft J, *J Pharm Sci,* **73**, 883–887(1984).
5. Albery W, Hadgraft J, *J Pharm Pharmacol,* **31**, 65–68(1979).
6. Lee G, Palicharla P, *Pharm Res,* **3**, 356–359(1986).
7. Kligman A, Christophers H, *Arch Dermatol,* **88**, 702–710(1963).
8. Tojo K, In: *Transdermal Controlled Systemic Medications,* Chien Y (ed), Marcel Dekker, New York, pp127–158(1987).
9. Spacek P, Kubin M, *J Poly Sci,* **C16**, 705–714(1967).
10. Crank J, Nicolson P, *Proc Camb Phil Soc,* **43**, 50–67(1947).
11. Göpferich A, Lee G, *Int J Pharm,* **71**, 245–253(1991).
12. Nelder J, Mead R, *Computer J,* **10**, 308–313(1967).
13. Michaels AS, Chandrasekaran SK, Shaw JE, *AIChE J,* **21**, 985–992(1975).
14. Tojo K, *J Pharm Sci,* **72**, 889–891(1987).
15. Crank J, *The Mathematics of Diffusion, 2nd Ed,* Oxford University Press, London, pp56–59(1975).
16. Arndts D, Arndts K, *Eur J Clin Pharmacol,* **26**, 79–85(1984).